

Supporting Information

Crystal structures and intense luminescence of tris(3-(2'-pyridyl)pyrazolyl)borate Tb³⁺ and Eu³⁺ complexes with carboxylate co-ligands.

*Elena A. Mikhalyova,^a Anastasiya V. Yakovenko,^a Matthias Zeller,^{b,c} Konstantin S. Gavrilenko,^d Mikhail A. Kiskin,^e Sergey S. Smola,^f Vladimir P. Dotsenko,^f Igor L. Eremenko,^e Anthony W. Addison,^{*g} & Vitaly V. Pavlishchuk^{*a}*

^a L. V. Pisarzhevskii Institute of Physical Chemistry of the National Academy of Sciences of the Ukraine, Prospekt Nauki 31, Kiev, 03028, Ukraine, tel. (38 044) 525 42 28, fax (38 044) 525 62 16, e-mail: shchuk@inphyschem-nas.kiev.ua;

^b STARBURSTT CyberInstrumentation Consortium and Department of Chemistry, Youngstown State University, One University Plaza, Youngstown OH 44555-3663, U.S.A.;

^c Department of Chemistry, Purdue University, 560 Oval Drive, West Lafayette, IN, 47907, U.S.A., e-mail: zeller4@purdue.edu;

^d Chembiocenter, Taras Shevchenko National University Of Kiev, Chervonotkatska, 61, 03022, Kiev, Ukraine.

^e N. S. Kurnakov Institute of General and Inorganic Chemistry, Russian Academy of Sciences, Leninsky Prosp. 31, 119991 Moscow, GSP-1, Russian Federation;

^f A.V. Bogatsky Physico-Chemical Institute of the National Academy of Sciences of the Ukraine, 86 Lustdorfskaya doroga, 65080 Odessa, Ukraine;

^g Department of Chemistry, Drexel University, Philadelphia, PA 19104-2816, U.S.A., e-mail: addisona@drexel.edu.

Single Crystal X-ray Diffraction. Data were collected using Bruker ApexII CCD or Quest CMOS diffractometers with Mo-K α radiation ($\lambda = 0.71073 \text{ \AA}$), or a Bruker AXS X8 Prospector CCD diffractometer with Cu-K α radiation. The ApexII instrument features a fine focus sealed tube X-ray source with graphite monochromator. The Quest CMOS and Prospector CCD instruments are equipped with I μ S microsources with a laterally graded multilayer (Goebel) mirror for monochromatization. Single crystals were mounted on Mitegen micromesh mounts using a trace of mineral oil and cooled in-situ to 100(2) K for data collection. Frames were collected, reflections were indexed and processed, and the files scaled and corrected for absorption using APEX2¹. The space groups were assigned and the structures were solved by direct methods using XPREP within the SHELXTL suite of programs² and refined by full matrix least squares against F^2 with all reflections using Shelxl2013 or 2014³ using the graphical interface Shelxle.⁴ If not specified otherwise H atoms attached to carbon and nitrogen atoms and hydroxyl hydrogens were positioned geometrically and constrained to ride on their parent atoms, with carbon hydrogen bond distances of 0.95 \AA for alkene and aromatic C-H, 1.00, 0.99 and 0.98 \AA for aliphatic C-H, CH₂ and CH₃, 0.88 for N-H and 0.84 \AA for OH moieties, respectively. Methyl and hydroxyl H atoms were allowed to rotate but not to tip to best fit the experimental electron density. $U_{\text{iso}}(\text{H})$ values were set to a multiple of $U_{\text{eq}}(\text{O/C/N})$ with 1.5 for CH₃ and OH, and 1.2 for C-H, CH₂ and N-H units, respectively. Complete crystallographic data, in CIF format, have been deposited with the Cambridge Crystallographic Data Centre. CCDC 1518607-1518619 contains the supplementary crystallographic data for this paper. These data can be obtained free of charge from The Cambridge Crystallographic Data Centre via www.ccdc.cam.ac.uk/data_request/cif.

Tp^{Py}Eu(CF₃CO₂)₂(H₂O) (3-Eu):

One of the trifluoro acetate ligands shows rotational disorder of the fluorine atoms. The atoms were refined as being disordered over two positions. The C-F distances were restrained to be similar and the minor occupied moiety CF₃ group to have

approximate tetrahedral geometry. ADPs of the F atoms were restrained to be approximately isotropic, and U_{ij} components of atoms were restrained to be similar. The occupancy ratio refined to 0.551(9) to 0.449(9). Disorder of one of the chloroform solvate molecules is observed. The molecule was refined as being disordered over three positions. The three molecules were restrained to have similar geometries and overlapping C and Cl atoms were constrained to have identical ADPs. The occupancy rates refined to 0.549(3), 0.354(3) and 0.098(2). One of the trifluoro acetate ligands is involved in the disorder and associated with the least occupied chloroform moiety. The minor occupied trifluoro acetate ligand was restrained to have a similar geometry as its major counterpart, to be flat, and equivalent atoms were constrained to have identical ADPs. The moiety was restrained from too closely approaching other non-disordered molecular fragments.

Tp^{Py}Tb(CCl₃CO₂)₂(H₂O) (4-Tb):

The structure is isotypic with its Eu analogue, was refined in a similar model as the Eu compound. The molecule shows systematic 1:1 disorder due to a close contact between H17 and its closest symmetry equivalent counterpart in a neighboring molecule. The disorder is most pronounced for the pyridyl-diazole unit H17, which is associated with shifts of over 0.7 Å. The disorder does however also extend to the two other diazole units, the Tb metal center, the coordinated water molecule and one of the trichloroacetate groups. The disordered sections were restrained to have similar geometries, and U_{ij} components of all disordered atoms were restrained to be similar for atoms closer to each other than 1.7 Å. The two Tb ions, the O atoms of the two water molecules, and the two C atoms of the disordered trichloroacetates were each constrained to have identical ADPs. The O atoms of the two water molecules were also restrained to be close to isotropic.

Tp^{Py}Eu(CCl₃CO₂)₂(H₂O) (4-Eu):

The structure is isotypic with its Tb analogue, was solved by isomorphous replacement and refined in the same model as the Tb compound. The molecule shows systematic 1:1 disorder due to a close contact between H17 and its closest symmetry

equivalent counterpart in a neighboring molecule. The disorder is most pronounced for the pyridyl-diazole unit H17, which is associated with shifts of over 0.7 Å. The disorder does however also extend to the two other diazole units and one of the trichloroacetate groups. The disordered sections were restrained to have similar geometries, and U_{ij} components of all disordered atoms were restrained to be similar for atoms closer to each other than 1.7 Å. The two C atoms of the disordered trichloroacetates were constrained to have identical ADPs.

Tp^{Py}Tb(C(CH₃)₃CO₂)₂(H₂O) (5-Tb):

One of the tert butyl groups is disordered over two positions. U_{ij} components of disordered atoms were restrained to be similar for atoms closer to each other than 1.7 Å. The occupancy ratio refined to 0.658(5) to 0.342(5). The solvating toluene molecule shows signs of partial disorder, but no obvious single second moiety could be defined and so no disorder was modeled for the toluene molecule.

Tp^{Py}Tb(C₆F₅CO₂)₂(H₂O) (8-Tb):

An acetonitrile solvent molecule was refined as disordered. U_{ij} components of disordered atoms were restrained to be similar for atoms closer to each other than 1.7 Å. The occupancy ratio refined to 0.711(14) to 0.289(14).

Tp^{Py}Eu(NA)₂(H₂O)·0.9CH₂Cl₂ (9-Eu·0.9CH₂Cl₂):

The population of CH₂Cl₂ molecule in the crystal of 9-Eu·0.9CH₂Cl₂ was defined from Fourier synthesis and then fixed.

(Tp^{Py}Eu)₂(pma)(MeOH)₂ (10-Eu):

Crystals rapidly desolvate upon being taken out of solution and break apart within seconds to less than a minute. Solvating methanol molecules are disordered over two alternative sets of positions. One set is associated with the presence of a water molecule, while the other misses that water molecule. The disorder extends to one of the keto oxygen atoms of the bridging ligand, and to the H atom of one of the coordinated methanol OH groups. For all disordered methanol molecules the C-O

distances were restrained to be similar, and U_{ij} components of all disordered atoms were restrained to be similar for disordered methanol and water atoms closer to each other than 1.7 Å. The disordered keto atoms were constrained to have identical ADPs, and to be close to isotropic, and their C-O distances were restrained to be similar. Water and hydroxyl H atom positions were restrained based on hydrogen bonding considerations. The occupancy ratio between the two sets of solvating molecules refined to 0.514(6) to 0.468(6).

(Tp^{Py}Tb)₂(pma)(MeOH)₂ (10-Tb)

Crystals rapidly desolvate upon being taken out of solution and break apart within seconds to less than a minute. Solvating methanol molecules are disordered over two alternative sets of positions. One set is associated with the presence of a water molecule, but the other misses that water molecule. The disorder extends to one of the keto oxygen atoms of the bridging ligand, and to the H atom of one of the coordinated methanol OH groups. For all disordered methanol molecules the C-O distances were restrained to be similar, and U_{ij} components of all disordered atoms were restrained to be similar for disordered methanol and water atoms closer to each other than 1.7 Å. The disordered keto atoms were constrained to have identical ADPs, and to be close to isotropic, and their C-O distances were restrained to be similar. Water and hydroxyl H atom positions were restrained based on hydrogen bonding considerations. The occupancy ratio between the two sets of solvating molecules refined to 0.542(8) to 0.458(8).

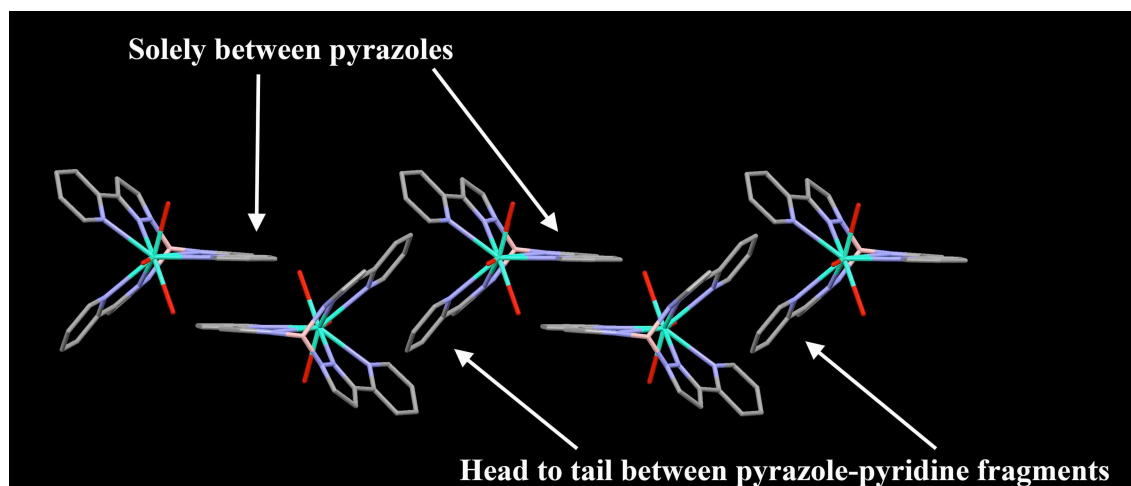


Figure S1. π -Stacking interactions between $[\text{Tp}^{\text{Py}}\text{Tb}(\text{H}_2\text{O})_3]^{2+}$ ions in the crystal lattice of $[\text{Tp}^{\text{Py}}\text{Tb}(\text{H}_2\text{O})_3]\text{Cl}_2$ (**1-Tb**).

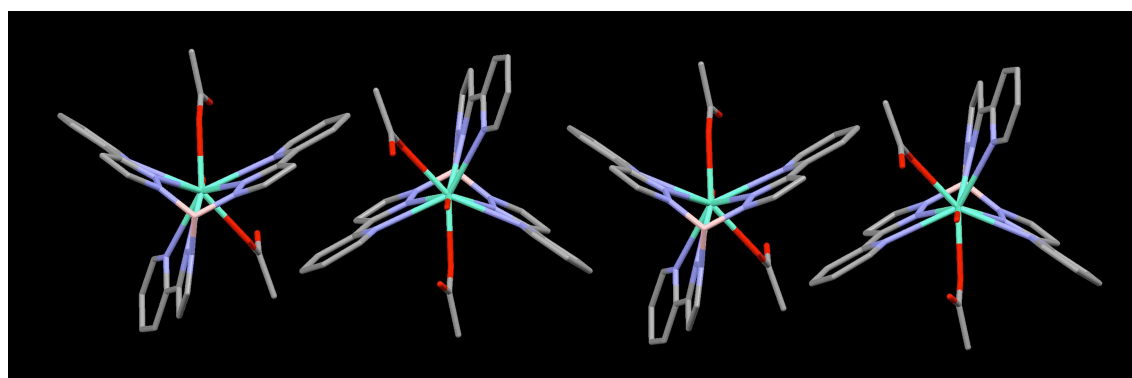


Figure S2. π -Stacking interactions between separate molecules in the $\text{Tp}^{\text{Py}}\text{Ln}(\text{CH}_3\text{CO}_2)_2(\text{H}_2\text{O})$ (**2-Ln**) lattice.

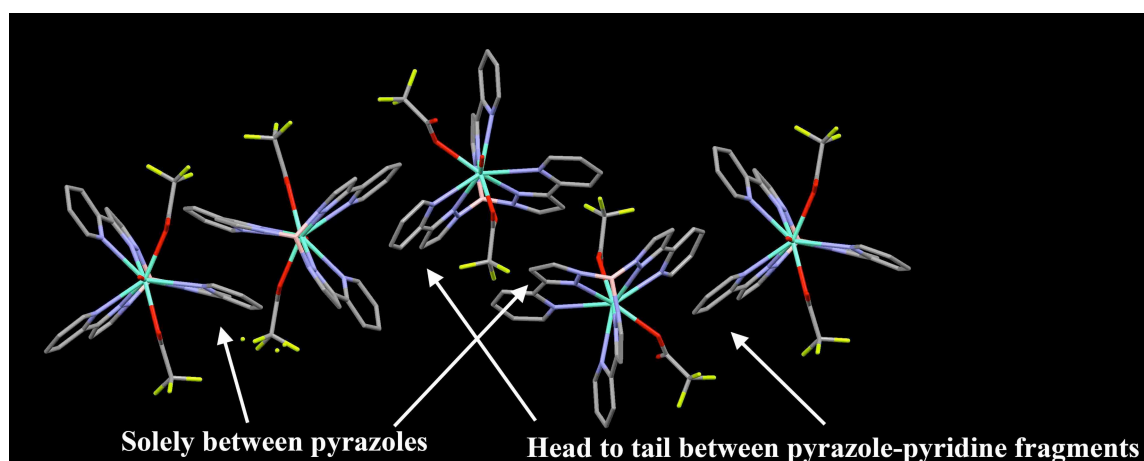


Figure S3. π -Stacking interactions between separate molecules in the $\text{Tp}^{\text{Py}}\text{Eu}(\text{CF}_3\text{CO}_2)_2(\text{H}_2\text{O})$ (**3-Eu**) lattice.

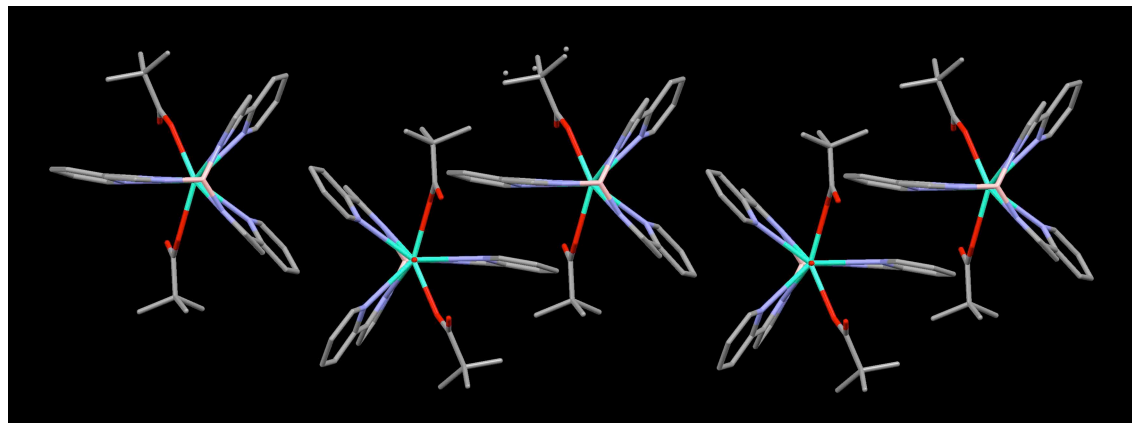


Figure S4. π -Stacking interactions between separate molecules in the $\text{Tp}^{\text{Py}}\text{Ln}(\text{C}(\text{CH}_3)_3\text{CO}_2)_2(\text{H}_2\text{O})$ (**5-Ln**) lattice.

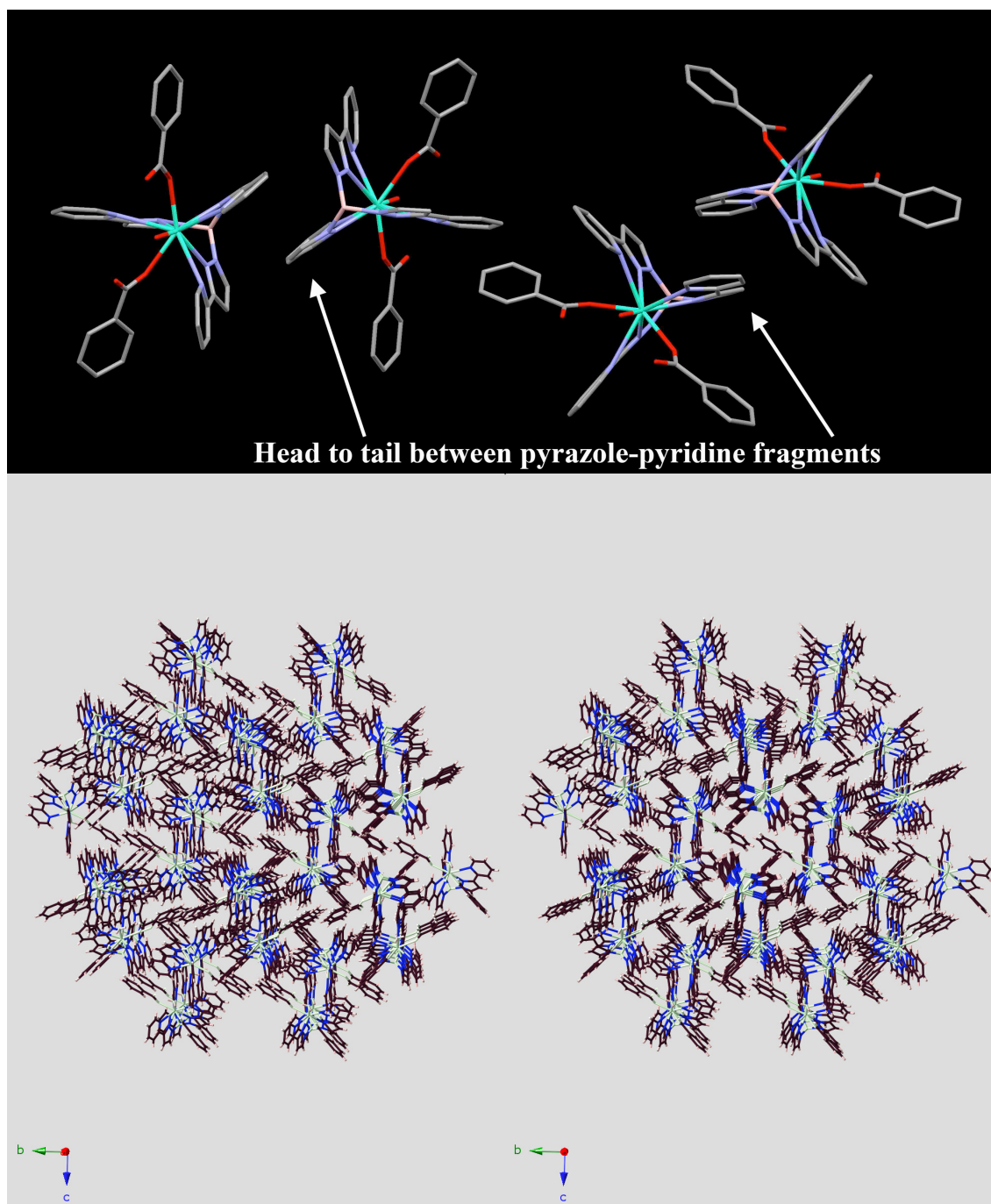


Figure S5. Stacking interactions between separate molecules in the crystal lattice of $\text{Tp}^{\text{Py}}\text{Tb}(\text{PhCO}_2)_2(\text{H}_2\text{O})$ (**7-Tb**) (upper); lattice view (inverse stereo, stick-structures) of $\text{Tp}^{\text{Py}}\text{Tb}(\text{PhCO}_2)_2(\text{H}_2\text{O})$ (**7-Tb**) (lower).

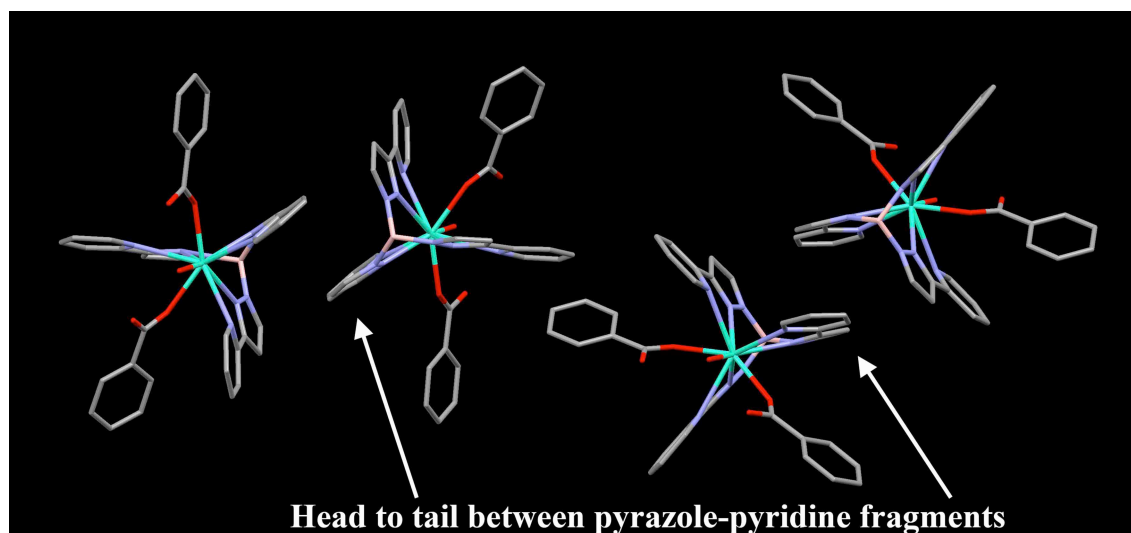


Figure S6. π -Stacking interactions between separate molecules in the $(\text{Tp}^{\text{Py}}\text{Ln})_2\text{pma}(\text{MeOH})_2$ (**10-Ln**) lattice.

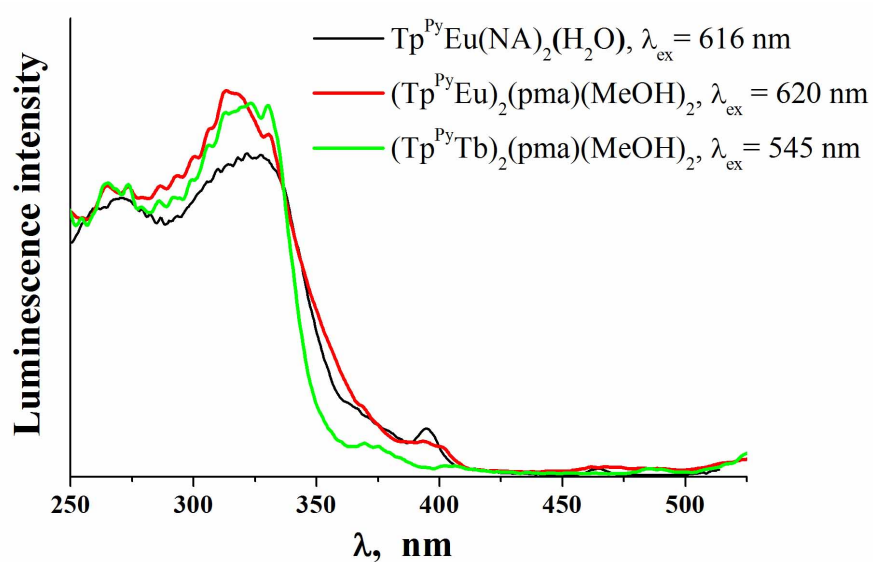


Figure S7. Excitation spectra (emission monitored at wavelengths shown on the figure) of $\text{Tp}^{\text{Py}}\text{Eu}(\text{NA})_2(\text{H}_2\text{O})$ (black), $(\text{Tp}^{\text{Py}}\text{Eu})_2(\text{pma})(\text{MeOH})_2$ (red) and $(\text{Tp}^{\text{Py}}\text{Tb})_2(\text{pma})(\text{MeOH})_2$ (green).

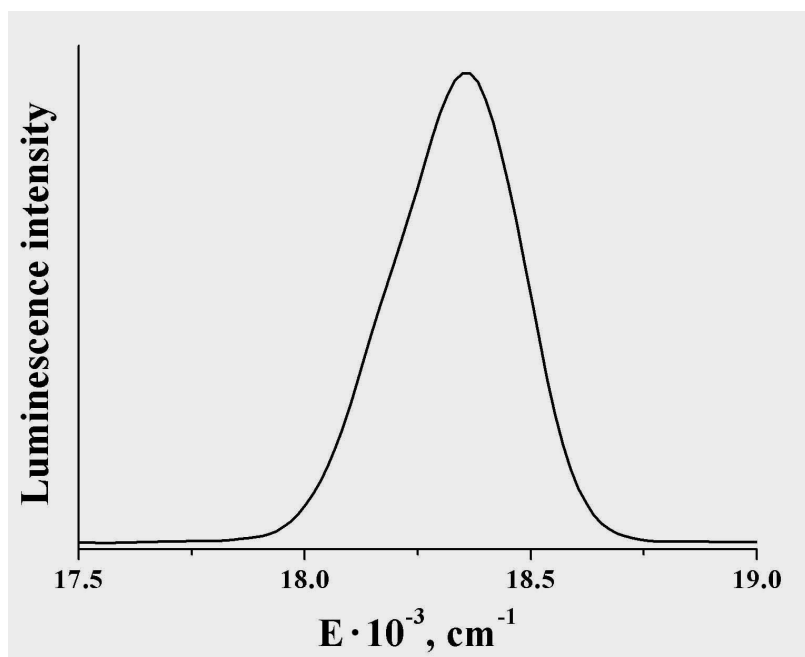


Figure S8. The non-symmetric shape of the ${}^5D_4 \rightarrow {}^7F_5$ emission band of $\text{Tp}^{\text{Py}}\text{Tb}(\text{Ad})_2(\text{H}_2\text{O})$.

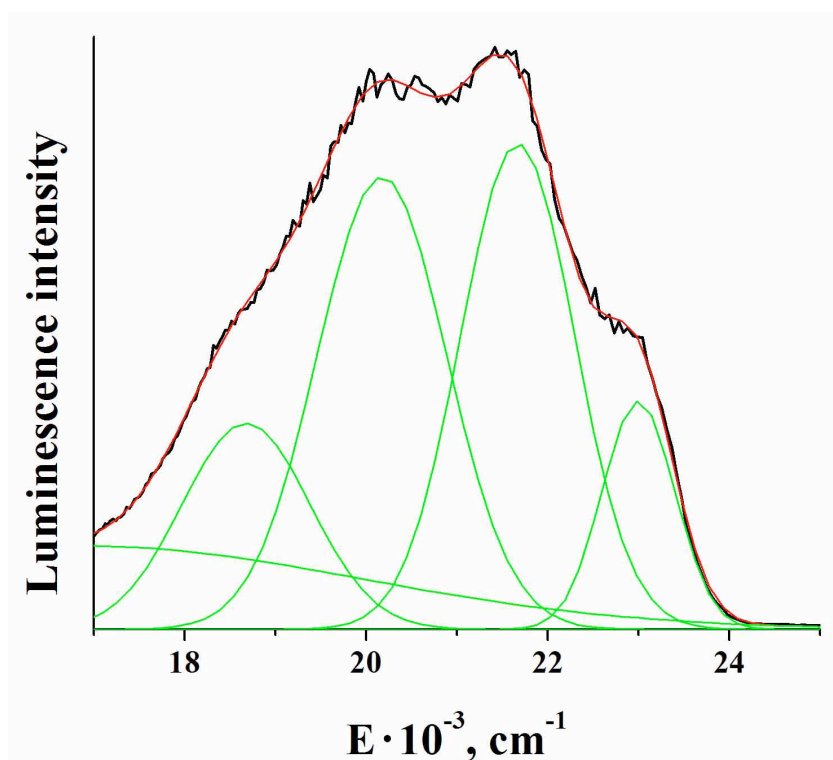


Figure S9. Solid-state phosphorescence emission spectrum of $\text{Tp}^{\text{Py}}\text{Gd}(\text{CH}_3\text{COO})_2(\text{H}_2\text{O})$ at 77K.

References

1. Apex2, Saint, Bruker AXS Inc.: Madison (WI), USA, 2014.

2. a) SHELXTL (Version 6.14) (2000-2003) Bruker Advanced X-ray Solutions, Bruker AXS Inc., Madison, Wisconsin: USA. b) G. M. Sheldrick, *Acta Cryst. A*, 2008, **64**, 112-122.
3. a) G. M. Sheldrick, *Acta Cryst. C*, 2015, **71**, 3-8. b) G. M. Sheldrick, (2013). University of Göttingen, Germany.
4. SHELXLE Rev656, Rev714 (Hübschle *et al.*, 2011), SHELXLE. C. B. Hübschle, G. M. Sheldrick, B. Dittrich, *J. Appl. Cryst.*, 2011, **44**, 1281-1284.